RSC Advances

RSC Publishing

COMMUNICATION

View Article Online
View Journal | View Issue

Effect of combination sequence of precursors on the structural and catalytic properties of Ti–SBA-15†

Cite this: *RSC Advances*, 2013, **3**, 12604

Received 19th March 2013,
Accepted 29th May 2013

DOI: 10.1039/c3ra41304g

www.rsc.org/advances

Feng-Ting Kuo,[a] Shih-Yuan Chen,[ab] Tsung-Han Lin,[a] Jyh-Fu Lee[c] and Soofin Cheng*[a]

The combination sequence of Ti and Si precursors (TTIP and TEOS) in the synthesis solution of Ti-incorporated SBA-15 mesoporous silica (shortly termed Ti–SBA-15) was found for the first time to be critical for the distribution of tetrahedrally (T_d) coordinated Ti(IV) sites in the resultant Ti–SBA-15. It was found that TTIP pre-assembled with P123 in the synthesis solution for 3 h before the addition of TEOS gave T_d-coordinated Ti(IV) sites predominately incorporated near the superficial regions of the framework and were highly accessible to the reactants in catalytic reactions.

1. Introduction

Ti-incorporated zeolitic materials, such as TS-1 and Ti–MWW, were reported to have remarkable catalytic activities in selective oxidation reactions using hydrogen peroxide as the oxidant at mild reaction temperatures.[1–5] However, the pore sizes of zeolitic materials are generally smaller than 1 nm and that limits their applications in sorption and reactions of bulky molecules. In the past two decades, many efforts have been devoted to the preparation of Ti-incorporated mesoporous silica materials because their relatively large pores facilitate the diffusion of bulky molecules often encountered in fine chemicals synthesis.[6–12]

Among the mesoporous materials, SBA-15 with pore diameters larger than 5 nm and a high hydrothermal stability, has attracted great attention.[13,14] Berube *et al.*[11] prepared well-ordered Ti–SBA-15 materials with Ti in T_d coordination up to a Ti/Si ratio of 5.6% by a controlled post-grafting method using a special Ti precursor of acetylacetone-chelated tetrapropylorthotitanate. However, the grafting method has shown to give poor control in the distribution of the active species.[15–17] Moreover, the complicated processing steps and solvent waste are other drawbacks in comparison to the co-condensation method. So far, the preparation of Ti–SBA-15 by one-pot co-condensation is a difficult task due to the incongruent hydrolysis and condensation rates of the silica and titania precursors, which are mainly tetraethyl orthosilicate (TEOS) and sodium silicate for silica, and titanium tetraisopropoxide (TTIP) and titanium(IV) chloride for titania.[6–8,12] Previous reports have indicated that mixed-phase products containing TiO_2 crystallites and disordered porous SiO_2 solids are frequently obtained by the co-condensation method.[7,8] Chen *et al.*[12] recently achieved evident success in preparing well-ordered Ti-incorporated SBA-15 with a superficially T_d-coordinated Ti species in a self-generated acidic environment (pH = 1–2) combined with calcination treatment. However, anatase TiO_2 nanoparticles which gave a negative effect on the selective oxidation reaction were found to co-exist in the materials.

In this study, the combination sequence of Ti and Si precursors in preparing Ti–SBA-15 materials by one-pot co-condensation in an acidic synthesis solution (1–2 M HCl) was examined. The results showed that the combination sequence markedly affected the Ti environment in SBA-15 and the catalytic properties of the resultant materials in the selected oxidation of 2,3,6-trimethylphenol (TMP) with H_2O_2.

2. Experimental

2.1 One-pot synthesized Ti–SBA-15

The Ti–SBA-15 materials were prepared by a co-condensation method based on the gel compositions of 0.017 P123 : 1 TEOS : 0.010–0.125 TTIP : 3.8–7.6 HCl : 210 H_2O. In the typical synthesis, 4.0 g of Pluronic P123 triblock copolymer (Aldrich, M_n = 5800) was thoroughly dissolved in 160 mL of 2 M HCl solution at 35 °C. To this solution, TTIP (Acros, 0.010–0.125 mol% of Si) was added and hydrolyzed for 3 h before the addition of 8.72 g of TEOS (Acros). The reaction mixture was sealed in a polypropylene bottle and stirred at 35 °C for 24 h, followed by hydrothermal treatment at 90 °C for another 24 h in a static condition. The solid precipitates were collected by filtration, washed with deionized

---

[a] Department of Chemistry, National Taiwan University, Taipei 10617, Taiwan E-mail: chem1031@ntu.edu.tw; Fax: +886-2-33668671; Tel: +886-2-33661662

[b] Research Center for New Fuels and Vehicle Technology, National Institute of Advanced Industrial Science and Technology, Tsukuba Central-5, 1-1-1 Higashi, Tsukuba, Ibaraki 305-8565, Japan

[c] Research Division, National Synchrotron Radiation Research Center, Hsinchu 300, Taiwan

† Electronic supplementary information (ESI) available: Fig. S1 and S2 small-angle XRD patterns; Fig. S3 wide-angle XRD patterns; Fig. S4 HRSEM of Ti–SBA-15. See DOI: 10.1039/c3ra41304g

water and dried, then were calcined at 560 °C in air for 6 h with a 1 °C $\min^{-1}$ ramping rate. The resultant materials were designated as *x*Ti–Si-*y*, where *x* is the Ti/Si molar percentage in the gels and *y* is the molarity of the HCl solution. For comparison, another series of Ti-incorporated SBA-15 materials, shortly termed *x*Si–Ti-*y*, were prepared based on the procedures of literature reports,[7,8] which were similar to those of *x*Ti–Si-*y* samples except that TEOS was pre-assembled with P123 micelles in the synthesis solution for 3 h before the addition of TTIP.

2.2 Characterizations

Powder X-ray diffraction (XRD) patterns were measured by a Philips X'pert Pro diffractometer using Cu-Kα radiation operated at 40 mA and 45 kV. The divergent slits of 1/32 and 1/2 were set for collecting small- and wide-angle XRD patterns, which showed 2θ regions of 0.5–5° and 15–80°, respectively. Nitrogen physisorption isotherms were measured by a Micromeritics Tristar 3000 instrument at liquid nitrogen temperature (77 K). Materials were degassed in vacuum (10^{-3} torr) for more than 6 h before the measurement. The specific surface area was calculated by the Brunauer–Emmett–Teller (BET) method in the P/P_0 region of 0.05–0.25. The pore size distributions (PSDs) were calculated by the Barrett–Joyner–Halenda (BJH) method using the desorption branch of the isotherm. The materials were photographed with a Hitachi S-800 Field Emission Scanning Electron Microscope (SEM), a JEOL JSM-7600F Field Emission Scanning Electron Microscope (FE-SEM) and a Hitachi H-7100 transmission electron microscope (TEM). Ti *K*-edge X-ray absorption spectra were obtained at the Beamline 17C of National Synchrotron Radiation Research Center (NSRRC) facility in Hsinchu, Taiwan. The standard operating conditions were 1.5 GeV and 350 mA. The photon energy was calibrated with a metallic Ti foil (*K*-edge, 4966 eV). The diffuse-reflectance (DR) UV-Vis spectra were obtained with a Hitachi U-3310 spectrometer equipped with an integrating sphere detector. Barium sulfate (Acros, 99 + %) was used as the reference. The elemental contents in the bulk were obtained by inductive-coupled plasma-mass spectrometry (ICP-MS) using a Perkin Elmer SCIEX ELAN 5000 ICP-MS instrument. Prior to measurement, the dried samples (*ca.* 20 mg) were dissolved in a mixed HF–HNO_3 solution and diluted to ppb level.

2.3 Catalytic reaction

Liquid phase oxidation of TMP ($C_9H_{12}O$, Acros, 99+ %) was carried out in a 3-necked round bottom flask (50 mL) connected to a water cooling condenser and a thermometer. The Ti-incorporated SBA-15 catalyst was pre-dried at 200 °C overnight. Typically, a solution of 0.16 g of TMP in 12 mL CH_3CN (Acros, 99+ %) was refluxed at 82 °C before adding 0.16 g of the catalyst and 0.408 g of H_2O_2 (Acros, 35%) as the oxidant. The TMP to catalyst weight ratio was kept at 1, and the H_2O_2/TMP molar ratio was kept *ca.* 3.5. The products were separated by HP6890 Gas Chromatography (GC) and qualitatively identified with a HP5973 mass selective detector. The quantitative analyses of the products were carried out by a Chrompack 9000 GC instrument equipped with a RTX-5 capillary column (60 m in length, 0.53 mm in diameter) and a flame ionization detector (FID), and toluene was used as an internal standard.

3. Results and discussion

3.1 Material characterization

The small-angle XRD patterns of the Ti-incorporated SBA-15 materials prepared by different combination sequences in 2 M HCl medium, namely *x*Ti–Si-2 and *x*Si–Ti-2, respectively, show three distinct diffraction peaks, corresponding to the (100), (110) and (200) planes of 2D hexagonal *p*6*mm* structure. They also show steep H_1 hysteresis loops at P/P_0 = 0.6–0.8, suggesting that both series of Ti-incorporated SBA-15 materials possess well-ordered and narrowly-distributed mesopores (Fig. S1 and S2, ESI†).[13] Moreover, no diffraction peaks of crystalline TiO_2 are observed in the wide-angle region (Fig. S3, ESI†), implying that Ti should be homogeneously incorporated in SBA-15.

Table 1, as well as Table S1 (ESI†), show that both series of Ti–SBA-15 materials have high surface areas (796–896 $m^2 g^{-1}$), large pore volumes (0.97–1.1 $cm^3 g^{-1}$) and ordered nanopores (*ca.* 6 nm), akin to those of conventional SBA-15 (entry 1). The Ti loadings in the solids were analyzed by ICP-MS technique, and only *ca.* 5–12.8 mol% of Ti in the synthesis solutions was incorporated in SBA-15. These results are consistent with previous reports that Ti is difficult to incorporate in mesoporous silica prepared in a strong acidic environment.[8] However, the *x*Ti–Si-2 samples (entries 2–6), prepared by assembling a Ti precursor with P123 micelles first, have slightly lower Ti loadings than *x*Si–Ti-2 (entries 7–11), which was prepared by adding a Si precursor first. For *x*Si–Ti-2 samples where TEOS is pre-hydrolyzed, the soft SBA-15 mesostructure is formed prior to the addition of the Ti precursor, TTIP. When TTIP is added, the condensation between Ti–OPr groups and silanol groups on the SBA-15 mesostructure would form Ti–O–Si bonds and Ti is incorporated into the silica matrix. In contrast, in *x*Ti–Si-2 samples where TTIP is pre-hydrolyzed first, the hydrolysis product $TiOCl_2$ is soluble in acid. The $TiOCl_2$ species, which interacts with P123 micelles before the addition of TEOS, is probably less effective when condensed with Si–OEt groups on TEOS. As a result, a lesser amount of Ti is incorporated into the silica framework of the *x*Ti–Si-2 samples.

The morphology and pore structure of these materials were photographed by high-resolution scanning electron microscopy (HRSEM) using a retarding technique (Fig. S4, ESI†). The HRSEM photos show that both series of Ti–SBA-15 materials are rod-like aggregates in the micrometer level. Indeed, all of the *x*Ti–Si-2 and *x*Si–Ti-2 samples with different Ti loadings have rod-like morphology 1–2 micrometers in size, similar to that of conventional SBA-15. The channeling pores are well-aligned along the long axis of the particles, and the pore mouths and concave channels are seen on the top of particles, which are the superficial features of mesoporous silica templated by block copolymers.[17–20]

Fig. 1 compares the DR UV-vis spectra of *x*Ti–Si-2 and *x*Si–Ti-2 materials. All the spectra possess an intense band centered at 205–209 nm, which is assigned to the ligand to metal charge transfer (LMCT) from O to isolated Ti in tetrahedral coordination.[4,12] The intensity of the O → Ti(T_d) LMCT increases with the Ti loadings, suggesting that more isolated Ti species are incorporated. When the Ti/Si ratio in gels is increased to *ca.* 8–12.5 mol%, two weak bands appear at *ca.* 240 and 300 nm. They are assigned to the LMCT from O to Ti in octahedral coordination and the band gap transition of TiO_2 nanocrystallites, respectively. These two bands

Table 1 Physicochemical and catalytic properties of 560 °C calcined *x*Ti–Si-2 and *x*Si–Ti-2 samples

		Ti/Si (mol%)				Product Select. (%)				
Entry	Materials	Gel	Solid	S_{BET} (m^2 g^{-1})	TMP conv.[a](%)	TMBQ	HTMBQ	TMCHT	BP	TOF[b](h^{-1})
1	SBA-15	0	0	801	5.3	0	0	0	100	0
2	2Ti–Si-2	2.0	0.10	858	12.4	24.5	0	0	75.5	3.3
3	4Ti–Si-2	4.0	0.40	874	23.2	51.1	0	0	48.9	3.3
4	5Ti–Si-2	5.0	0.70	813	47.7	48.3	9.9	2.0	39.8	3.6
5	8Ti–Si-2	8.0	1.0	824	65.8	51.9	9.6	3.6	34.9	3.8
6	12.5Ti–Si-2	12.5	1.6	810	92.0	68.2	4.5	3.0	24.3	4.3
7	12.5Ti–Si-2[c]	—	—	—	93.2	69.1	3.5	2.4	25.0	—
8	Recycl. 12.5Ti–Si-2[d]	—	—	—	91.5	67.3	3.5	3.2	26.0	—
9	2Si–Ti-2	2.0	0.40	796	36.1	0	0	0	100	0
10	4Si–Ti-2	4.0	0.70	837	45.7	39.1	1.2	1.2	58.5	2.8
11	5Si–Ti-2	5.0	0.90	799	53.7	41.5	12.6	2.8	42.5	2.7
12	8Si–Ti-2	8.0	1.4	870	57.5	50.3	10.5	8.3	30.4	2.3
13	12.5Si–Ti-2	12.5	2.8	896	60.1	60.4	7.6	14.8	17.2	1.4
14	12.5Si–Ti-2[c]	—	—	—	57.3	61.8	5.6	13.2	19.4	—
15	Recycl.12.5Si–Ti-2[d]	—	—	—	56.8	61.3	6.2	14.5	18.0	—

[a] Reaction conditions: 82 °C, 4 h, 0.16 g catalyst, 0.16 g TMP, 0.408 g H_2O_2 (35 wt%), 12 mL CH_3CN. [b] Molar yield of TMBQ per mole of Ti in the first hour. [c] New batches of samples. [d] The catalyst of the new batch of sample was regenerated by calcination at 500 °C for 3 h with a ramping rate of 1 °C min^{-1}.

on the *x*Si–Ti-2 series are more intense than those of the *x*Ti–Si-2 series, when comparing materials of the same Ti/Si ratios in the synthesis gels. Elemental analyses show that the Ti loadings in the solids giving 240 and 300 nm bands are 1–2.8 mol%. These results imply that the maximum Ti/Si ratio in Ti–SBA-15 materials to retain Ti in a T_d coordination geometry should be lower than 1 mol%.

The Ti loadings in Ti–SBA-15 products can be increased up to 4.4–5.1 mol% by using 1–1.5 M HCl instead of 2 M HCl to reduce the acidity of the synthesis solution. Table 2 shows that the materials thus prepared by assembling the Ti precursor with P123 micelles first still have well ordered mesostructures, high surface areas (>835 m^2 g^{-1}) and pore volumes (>1.00 cm^3 g^{-1}). However, the DR UV-vis spectra (Fig. S5, ESI†) show that the bands corresponding to TiO_2 nanocrystallites at *ca.* 240 and 300 nm are more easily detected, especially in the synthesis condition of higher pH values. The UV-vis spectra can retain low intensity in this region when the Ti/Si ratio in the synthesis gels is lower than 5% using 2 M HCl, while that decreases to 4% with 1.5 M HCl and to 2% with 1 M HCl. Under these Ti/Si ratios, the Ti loadings in the solid products do not exceed 1 mol% based on ICP-MS analysis (Tables 1 and 2). These results suggest that the maximum amount of Ti which can substitute the framework Si in SBA-15 prepared by one-pot co-condensation should be *ca.* 1 mol%, and that value is not significantly influenced by the acidity of the synthesis solutions. Above this ratio, Ti has the tendency to form TiO_2 nanocrystallites.

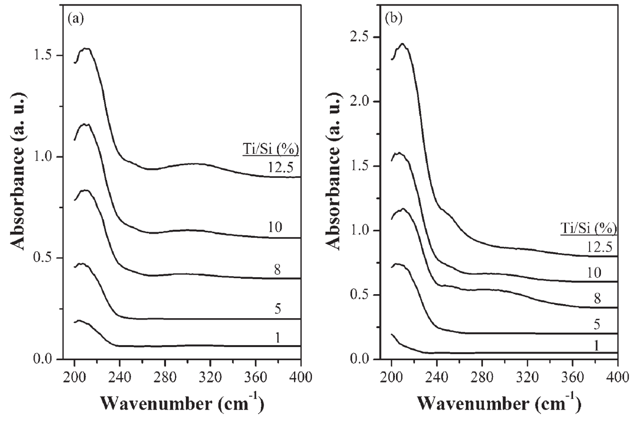

Fig. 1 DR UV-vis spectra of 560 °C calcined samples: (a) *x*Ti–Si-2 and (b) *x*Si–Ti-2.

The chemical environments of Ti(IV) species in both series of Ti-incorporated SBA-15 materials prepared using 2 M HCl were examined by Ti *K*-edge X-ray absorption near edge structure (XANES) spectroscopy at beamline 17C of NSRRC, Hsinchu, Taiwan. Samples 12.5Ti–Si-2 and 12.5Si–Ti-2 were selected because they have relatively high loadings of Ti meaning that their Ti *K*-edge X-ray absorption spectra are more clearly resolved. Moreover, the UV-vis spectra of these samples illustrate that the majority of the Ti species are in T_d-coordination. These XANES spectra are compared with that of anatase TiO_2 (JRC-TIO-1 of Japan Reference Catalysts), as shown in Fig. 2. For anatase TiO_2, three main-features of B (4980 eV), C_1 (4987 eV) and D (5004 eV) are attributed to the electron transition from an initial state of the Ti 1s energy level to the excited states of the predominately Ti 4p energy level, and three pre-edge features of A_1 (4969 eV), A_2 (4971 eV) and A_3 (4974 eV) are due to the electron transition from the Ti 1s energy level to bound 3d (or O 2p) molecular orbitals.[12,20–25] Since Ti in anatase TiO_2 is in octahedral (O_h) coordination and has the center of symmetry, the 1s → 3d transition is Laporte forbidden. That accounts for the weak intensity of the pre-edge features.

The Ti *K*-edge XANES spectrum of calcined 12.5Ti–Si-2 material resembles that of anatase TiO_2, indicating that most of the Ti species in this sample are in O_h coordination. However, when the calcined 12.5Ti–Si-2 sample was dehydrated at 200 °C in vacuum

Table 2 Physicochemical and catalytic properties of 560 °C calcined *x*Ti–Si-1.5 and *x*Si–Ti-1.5 samples

	Ti/Si (mol%)				Product Select. (%)				
Materials	Gel	Solid	S_{BET} (m^2 g^{-1})	TMP conv.^{a}(%)	TMBQ	HTMBQ	TMCHT	BP	TOF^b(h^{-1})
1Ti–Si-1	1	0.2	927	20.1	21.5	0	0	78.5	2.4
2Ti–Si-1	2	0.7	986	54.0	46.3	18.9	5.9	28.9	3.9
4Ti–Si-1	4	1.0	923	59.0	54.9	15.1	9.6	20.4	3.6
5Ti–Si-1	5	1.8	932	75.2	57.9	11.9	11.6	18.6	2.7
8Ti–Si-1	8	3.4	867	25.0	32.5	0	3.5	64	0.3
10Ti–Si-1	10	5.1	864	17.1	0	0	0	100	0
1Ti–Si-1.5	1	0.08	900	7.0	0	0	0	100	0
2Ti–Si-1.5	2	0.2	911	9.2	9.8	0	0	90.2	0.5
4Ti–Si-1.5	4	0.9	915	60.3	62.3	12.9	16.1	8.7	4.6
5Ti–Si-1.5	5	1.1	930	67.3	65.9	19.0	11.4	3.7	4.4
8Ti–Si-1.5	8	2.6	835	64.7	48.9	11.0	8.2	31.9	1.3
10Ti–Si-1.5	10	4.4	884	32.7	32.1	14.7	4.3	48.9	0.3

[a] Reaction conditions: 82 °C, 4 h, 0.16 g catalyst, 0.16 g TMP, 0.408 g H_2O_2 (35 wt%), 12 mL CH_3CN. [b] Molar yield of TMBQ per mole of Ti in the first hour.

for 8 h, the three pre-edge A features are replaced by a relatively strong peak centered at *ca.* 4970.2 eV. The pre-edge peak of the 1s → 3d transition becomes intense when the selection rule is released, which means that the Ti atom no longer has the center of symmetry. In other words, the pre-edge feature suggests that the Ti species in the dehydrated 12.5Ti–Si-2 material are most likely to be at the tetrahedral center, and that can occur only when Ti is substituting the Si sites on the silica framework. Moreover, these T_d-coordinated Ti sites readily coordinate with water molecules from a humid atmosphere to form O_h-coordinated Ti species, and the process is reversible upon dehydration. These results are the evidence that most of the Ti incorporated in the 12.5Ti–Si-2 material, prepared by adding Ti first, is located near the superficial regions of the pore walls.

The Ti *K*-edge XANES spectra of the calcined 12.5Si–Ti-2 material, prepared by adding Si first, and that after dehydration at 200 °C for 8 h have only one intense pre-edge peak (Fig. 2(d) and (e)), implying that a large portion of the Ti species in 12.5Si–Ti-2 material are in a T_d coordination. Since these Ti sites are insensitive to moisture and dehydration, they are likely in the inner regions of the SBA-15 framework and not easily accessed by water molecules.

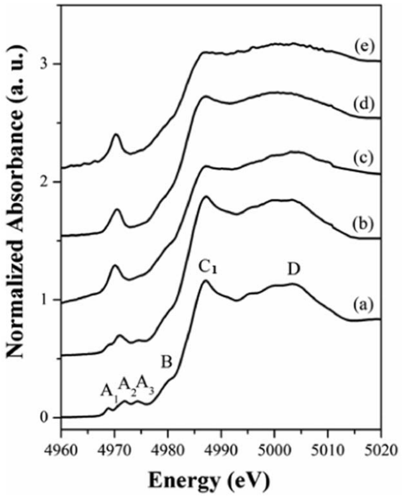

Fig. 2 Ti *K*-edge XANES spectra of (a) anatase TiO_2, (b) calc. 12.5Ti–Si-2, (c) dehyd. 12.5Ti–Si-2, (d) calc. 12.5Si–Ti-2, and (e) dehyd. 12.5Si–Ti-2.

3.2 Catalytic studies

In order to examine the catalytic performance of Ti-incorporated SBA-15 materials prepared by a different combination sequence of Ti and Si precursors, selective oxidation of TMP with H_2O_2 was studied as the model reaction. The targeting product is 2,3,6-trimethylbenzoquinone (TMBQ), an important intermediate for the synthesis of Vitamin E. The by-products are 2,2′-3,3′-5,5′-hexamethyl-4,4-biphenol (BP), 2-hydroxyl-3,5,6,-trimethyl-benzoquinone (HTMBQ), and 3,5,6-trimethyl-cyclohex-5-ene-1,2,4-trione (TMCHT), as shown in Scheme 1. Fig. 3 shows the selective oxidation of TMP with H_2O_2 in CH_3CN at 82 °C as a function of time over the 12.5Ti–Si-2 material. The TMP conversion rapidly reaches 92% at 4 h and retains the value thereafter, while the TMBQ yield increases continuously up to 82% in 7 h. These results imply that there are side products other than TMBQ formed. By tracing the distribution of by-products as a function of time, it is found that BP appears rapidly at the early stage, grows to an appreciable concentration during 1–4 h, and then gradually decreases with time and almost disappears after 7 h. In contrast, the amount of HTMBQ and TMCHT is negligible at the beginning of the reaction, and their yields increase with reaction time. HTMBQ and TMCHT are considered to be produced by further oxidation of TMBQ. Since BP is formed by dimerization of two TMP molecules, BP should be a parallel product of TMBQ. The observation of the maximum yield of BP during the reaction period is elucidated by that dimerization of TMP to form BP is a reversible reaction. BP is consumed as the TMP is used up in oxidation to form TMBQ.[26] For the purpose of comparing the catalytic activities of the Ti-incorporated SBA-15 materials prepared by varying the combination sequences of Ti and Si precursors, the results of the catalytic reaction after 4 h are compared hereafter.

The catalytic results over the two series of Ti–SBA-15 materials prepared in 2 M HCl are tabulated in Table 1, and the graphic

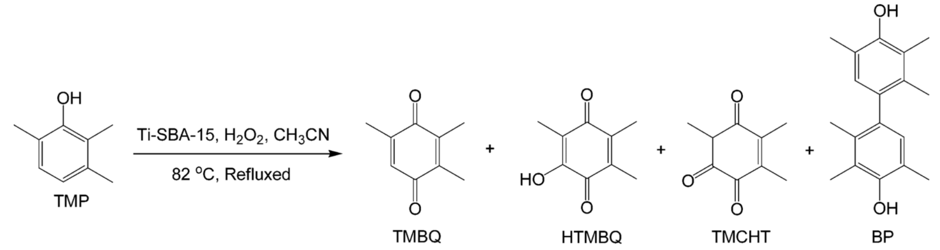

Scheme 1 Liquid phase oxidation of TMP with H_2O_2 catalyzed by Ti-incorporated SBA-15 materials.

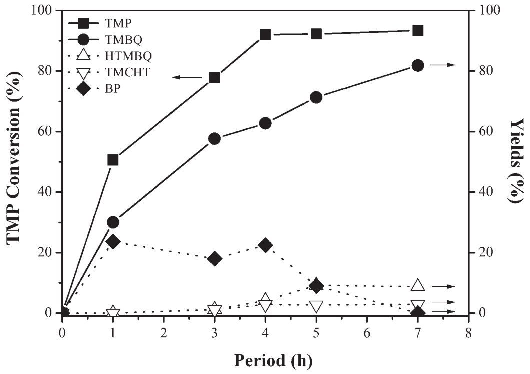

Fig. 3 Selective oxidation of TMP with H_2O_2 as a function of time over the calcined 12.5Ti–Si-2 material.

correlations of the catalytic performances as a function of Ti loadings in the solids are shown in Fig. 4. Siliceous SBA-15 gives a very low activity in the oxidation of TMP with H_2O_2, and BP is the only product obtained. Both *x*Ti–Si-2 and *x*Si–Ti-2 series materials can efficiently catalyze the oxidation of TMP with H_2O_2 to form TMBQ, except catalyst 2Si–Ti-2. The TMP conversion and TMBQ selectivity increase with Ti loading, while the BP selectivity varies in the reverse trend. Since UV-vis spectra show the amount of T_d-coordinated Ti species increases with the Ti loading in these Ti–SBA-15 materials, the T_d-coordinated Ti should be the main active site for selective oxidation of TMP to form TMBQ. A possible mechanism has been proposed by Kholdeeva *et al.*[26] to explain that high surface Ti(IV) concentration in T_d coordination is favourable for TMBQ formation, while low T_d-coordinated Ti(IV) concentration will lead to high BP selectivity. The *x*Ti–Si-2 series always gives higher TMBQ selectivities than the *x*Si–Ti-2 series when comparing samples with similar Ti content in the solids. It is an indication that the *x*Ti–Si-2 catalysts should have more T_d-coordinated Ti(IV) species on the superficial region.

The TOF is defined as the initial TMBQ yield per Ti site in the first hour, and a higher TOF value infers the better accessibility of the T_d-coordinated Ti sites in the catalysts. The TOFs of *x*Ti–Si-2 catalysts are around 3.3–4.3 h^{-1}, and the values slightly increase

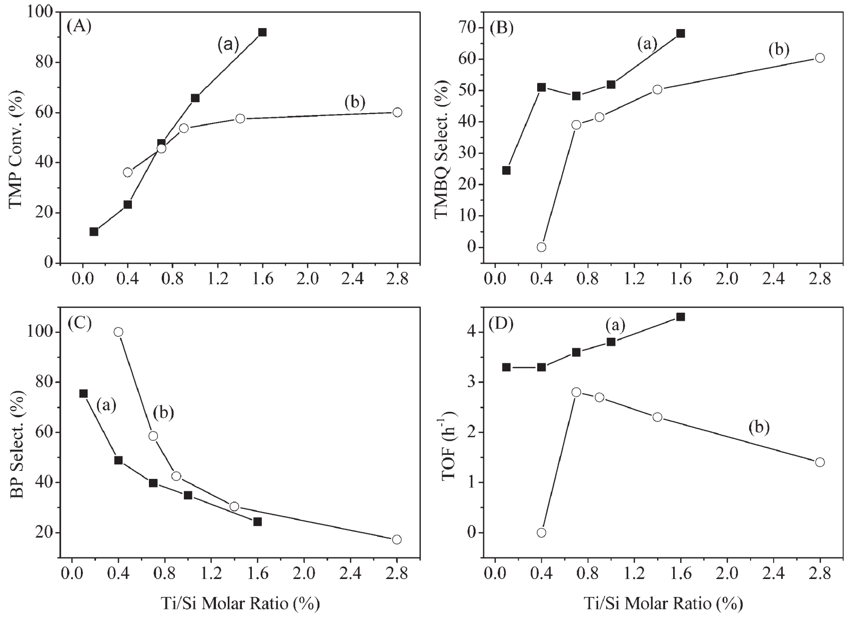

Fig. 4 Graphic correlation of catalytic performances (A) TMP conversion, (B) TMBQ selectivity and (C) BP selectivity after 4 h, and (D) TOF in the first hour of TMP oxidation with H_2O_2 at 82 °C, as a function of Ti loadings in Ti–SBA-15 materials prepared in 2 M HCl: (a) *x*Ti–Si-2 prepared by adding the Ti precursor first, and (b) *x*Si–Ti-2 prepared by adding the Si precursor first.

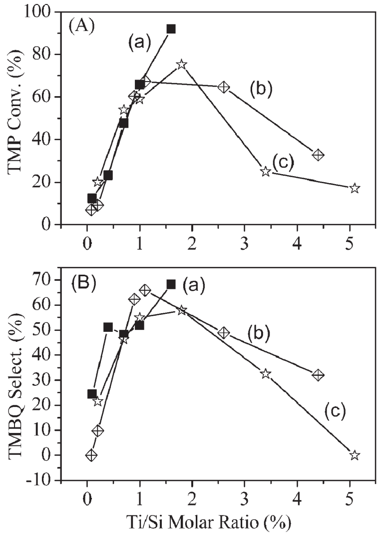

Fig. 5 Graphic correlation of catalytic performances (A) TMP conversion and (B) TMBQ selectivity in TMP oxidation with H_2O_2 at 82 °C, 4 h as a function of Ti loadings in Ti–SBA-15 materials prepared by pre-assembly of P123 micelles and TTIP for 3 h before the addition of TEOS in (a) 2 M, (b) 1.5 M, and (c) 1 M HCl.

with the increase in Ti loading up to the maximal Ti/Si ratio of 1.6 mol%. It is noticeable that the *x*Si–Ti-2 catalysts, which have relatively higher Ti content, give lower TOFs of 1.4–2.8 h^{-1}. The maximal TOF is achieved over 4Si–Ti-2, and the TOF value decreases almost linearly with further increase of Ti loading in *x*Si–Ti-2 catalysts. These results should be due to the fact that a large portion of the Ti sites in the *x*Si–Ti-2 series materials are not accessible by the reactants. That is consistent with the observation on Ti *K*-edge XANES spectra. In contrast, the higher TOFs of *x*Ti–Si-2 catalysts prepared by adding the Ti precursor first are due to the higher accessibility of T_d-coordinated Ti(IV) sites on the superficial region of the SBA-15 framework.

Entries 6 and 7 of 12.5Ti–Si-2, as well as entries 13 and 14 of 12.5Si–Ti-2 in Table 1 are different batches of materials prepared by different students. The similarity in catalytic performances of the materials from different batches demonstrates that the materials are easily reproduced. The used catalysts are regenerated by calcination at 500 °C for 3 h. The catalytic results of the recycling catalysts shown in entries 8 and 15 illustrate that the catalytic activities of these Ti–SBA-15 materials can be well retained.

The Ti contents in the solids can be further increased to 4–5 mol% by lowering the acid concentrations using 1–1.5 M HCl in the synthesis solutions (Table 2), yet the highest TMP conversions and TMBQ selectivities are obtained from the samples with Ti loadings in the solids around 1.1–1.8 mol% (Fig. 5). Indeed, the UV-vis spectra show that these materials contain the highest amount of T_d-coordinated Ti species in these two series of samples. Although both *x*Ti–Si-1 and *x*Ti–Si-1.5 materials were also prepared by adding the Ti precursor first and the Ti(IV) ions are supposed to locate at superficial regions of SBA-15 framework, relatively large amounts of TiO_2 crystallites are formed when the synthesis solutions are of higher pH values. Based on these results, 2 M HCl is favourable to 1–1.5 M HCl in preparing catalytically active Ti–SBA-15 materials.

4. Conclusions

The present studies demonstrate that pre-assembly of P123 micelles and the Ti precursor, TTIP, for 3 h before the addition of the Si precursor TEOS in synthesizing Ti–SBA-15 is important in preparing Ti–SBA-15 materials with more T_d-coordinated Ti(IV) dispersed on the superficial regions of the pore walls. These T_d-coordinated Ti(IV) centers are highly accessible by the reactants, and they contribute to the high catalytic activities of the Ti–SBA-15 materials in liquid phase oxidation of TMP with H_2O_2 to form TMBQ. In contrast, more Ti(IV) ions are hidden in the inner regions of the SBA-15 framework and lose their accessibility to the reactants in conventional Ti–SBA-15 prepared by pre-assembling P123 and the Si precursor before the addition of the Ti precursor. These results demonstrate the importance of a combination sequence in preparing catalytically active metal-substituted mesoporous materials. The used Ti–SBA-15 catalysts can be easily regenerated by calcination at 500 °C for 3 h, and the recycling catalysts were found to retain their catalytic activities well.

Acknowledgements

This work was supported by the National Science Council and Ministry of Education, Taiwan. Acknowledgements were also extended to C. Y. Tang, C. Y. Lin and S. J. Ji of Instrumentation Center, National Taiwan University for EM measurement.

References

1 M. A. Uguina, D. P. Serrano, G. Ovejero, V. Grieken and M. Camacho, *Appl. Catal., A*, 1995, **124**, 391.

2 G. Tozzola, M. A. Mantegazza, G. Ranghino, G. Petrini, S. Bordigay, G. Ricchiardiy, C. Lambertiy, R. Zuliany and A. Zecchina, *J. Catal.*, 1998, **179**, 64.

3 S. C. Laha and R. Kumar, *J. Catal.*, 2002, **208**, 339.

4 W. Fan, R. G. Duan, T. Yokoi, P. Wu, Y. Kubota and T. Tatsumi, *J. Am. Chem. Soc.*, 2008, **130**, 10150.

5 F. Song, Y. Liu, H. Wu, M. He, P. We and T. Tatsumi, *J. Catal.*, 2006, **237**, 359.

6 B. L. Newalker, J. Clanrewaju and S. Komarneni, *Chem. Mater.*, 2001, **13**, 552.

7 W. H. Zhang, J. Lu, B. Han, M. Li, J. Xiu, P. Ying and C. Li, *Chem. Mater.*, 2002, **14**, 3413.

8 Y. Chen, Y. Huang, J. Xiu, X. Han and X. Bao, *Appl. Catal., A*, 2004, **273**, 185.

9 K. Lin, P. P. Pescarmona, K. Houthoofd, D. Liang, G. V. Tendeloo and P. A. Jacobs, *J. Catal.*, 2009, **263**, 75.

10 T. Yokoi, T. Karouji, S. Ohta, J. N. Kondo and T. Tatsumi, *Chem. Mater.*, 2010, **22**, 3900.

11 F. Berube, B. Nohair, F. Kleitz and S. Kaliaguine, *Chem. Mater.*, 2010, **22**, 1988.

12 S. Y. Chen, C. Y. Tang, J. F. Lee, L. Y. Jang, T. Tatsumi and S. Cheng, *J. Mater. Chem.*, 2011, **21**, 2255.

13 D. Zhao, J. Feng, Q. Huo, N. Melosh, G. H. Fredrickson, B. F. Chmelka and G. D. Stucky, *Science*, 1998, **179**, 548.

14 S. Y. Chen and S. Cheng, *Chem. Mater.*, 2007, **19**, 3041.

15 L. H. Hsiao, S. Y. Chen, S. J. Huang, S. B. Liu, P. H. Chen, J. C. C. Chan and S. Cheng, *Appl. Catal., A*, 2009, **359**, 96.
16 S. Y. Chen, J. F. Lee and S. Cheng, *J. Catal.*, 2010, **270**, 196.
17 S. Y. Chen, T. Yokoi, C. Y. Tang, L. Y. Jang, T. Tatsumi, J. C. C. Chan and S. Cheng, *Green Chem.*, 2011, **13**, 2920.
18 S. Che, K. Lung, T. Tatsumi, S. Iijiima, H. Joo, R. Ryoo and O. Terasaki, *Angew. Chem., Int. Ed.*, 2003, **42**, 2182.
19 A. Endo, M. Yamada, S. Kataoka, T. sano, Y. Jnagi and A. Miyaki, *Colloids Surf., A*, 2010, **357**, 11.
20 S. Y. Chen, C.-Y. Hung, T. Yokoi, C.-T. Tang, S.-J. Huang, J. J. Jau, J. C. C. Chan, T. Tatsumi and S. Cheng, *J. Mater. Chem.*, 2012, **22**, 2233.
21 Z. Y. Wu, G. Ouvrard, P. Gressier and C. R. Natoli, *Phys. Rev. B: Condens. Matter*, 1997, **55**, 10382.
22 D. Cabaret, Y. Joly, H. Renevier and C. R. Natoli, *J. Synchrotron Radiat.*, 1999, **6**, 258.
23 F. Farges, G. E. Brown and J. J. Rehr, *Phys. Rev. B: Condens. Matter*, 1997, **56**, 1809.
24 J. M. Fraile, J. Garcya, J. A. Mayoral, M. G. Proietti and M. C. Sanchez, *J. Phys. Chem.*, 1996, **100**, 19484.
25 M. Bandyopadhyay, A. Birkner, M. W. E. van den Berg, K. V. Klementiev, W. Schmidt, W. Grunert and H. Gies, *Chem. Mater.*, 2005, **17**, 3820.
26 O. A. Kholdeeva, I. D. Ivanchikova, M. Guidotti, N. Ravasio, M. Sgobba and M. V. Barmatova, *Catal. Today*, 2009, **141**, 330.